

## Semiconductor to metal transition in PbS nanowires grown in mica channels

P. K. Mukherjee, K. Chatterjee, and D. Chakravorty

*Unit on Nano Science & Technology, Indian Association for the Cultivation of Science, Kolkata, 700 032, India*

(Received 7 June 2005; revised manuscript received 28 October 2005; published 9 January 2006)

It has been possible to grow PbS nanowires of diameter 1.2 nm within the crystal channels of Na-4 Mica. These nanowires exhibit a semiconductor to metal transition at  $\sim 300$  K as the temperature is lowered. Generation of pressure around 3 GPa on these wires due to a thermal expansion mismatch of Na-4 Mica and PbS phases is believed to cause this transition. A nonlinear voltage current characteristics at different temperatures is ascribed to the formation of nanojunctions between the metallic phases and not transformed PbS regions. The semiconductor-metal transition at 300 K is accompanied by a transition from a low to a high dielectric constant. The large value of dielectric constant shown by the nanocomposites is explained as arising due to the Rice-Bernasconi mechanism of dielectric polarizability in broken one-dimensional conductors.

DOI: [10.1103/PhysRevB.73.035414](https://doi.org/10.1103/PhysRevB.73.035414)

PACS number(s): 73.22.-f, 81.07.Bc, 81.07.Vb, 81.20.Fw

### INTRODUCTION

One-dimensional nanostructures have received considerable attention in recent years because of the interesting physical properties exhibited by them.<sup>1-8</sup> Metallic as well as semiconducting nanowires were grown by either using a template or under suitable chemical environment.<sup>9-11</sup> We have recently shown that metallic (silver) nanowires can be grown within the crystal channels of fluorophlogopite mica.<sup>12</sup> The composites exhibit ultrahigh dielectric permittivity which can be explained on the basis of Gorkov-Eliashberg<sup>13</sup> and Rice-Bernasconi<sup>14</sup> theoretical models. The model of Gorkov and Eliashberg deals with the calculation of the electronic susceptibility of a macroscopic system of discrete energy levels. They had followed up the work of Kubo<sup>15</sup> who showed that a metallic particle of very small diameter would have discrete electronic energy levels. Their theoretical prediction was that the electronic polarizability of the latter should be enormously large as compared to the polarizability estimated on the basis of elementary electrostatics. However, several carefully conducted experiments to confirm the above prediction proved futile.<sup>16,17</sup> This was ascribed to the canceling effect of the depolarization field due to the spherical geometry of the particle.<sup>14</sup> The Rice-Bernasconi model, on the other hand, is based on the presence of quasi-one-dimensional metals consisting of interrupted strands. Discretization of electronic energy levels is ensured in such a situation, but the difficulty associated with a depolarization field is removed. PbS is an important semiconducting material which is used in infrared detectors. We have grown PbS nanowires of diameter  $\sim 1.2$  nm in the channels of a high-charge density sodium fluorophlogopite mica of the chemical composition  $\text{Na}_4\text{Mg}_6\text{Al}_4\text{Si}_4\text{O}_{20}\text{F}_4 \cdot x \text{H}_2\text{O}$ .<sup>18</sup> These nanowires exhibit a semiconductor to metal transition at a temperature around 300 K. The details are reported in this paper.

### EXPERIMENT

The synthesis of the mica of the above-mentioned composition and commonly referred to as Na-4 mica was done

by the sol-gel method. The precursors used were  $\text{Al}(\text{NO}_3)_3 \cdot 9 \text{H}_2\text{O}$  and  $\text{Mg}(\text{NO}_3)_2 \cdot 6 \text{H}_2\text{O}$  and tetraethylorthosilicate. These were dissolved in ethyl alcohol and the solution stirred for 3 h. The amounts taken were such that a target composition  $3 \text{MgO} \cdot \text{Al}_2\text{O}_3 \cdot 2 \text{SiO}_2$  could be achieved after gelation and calcination. The gel was dried at 373 K and calcined at 748 K for 12 h. The gel powder was ground and mixed intimately with an equal amount of NaF powder. The mixture was heated at 1163 K for 18 h in a platinum crucible under ordinary atmosphere. The reaction products were first washed with de-ionized water and then with saturated boric acid. These were subsequently washed with 1 M NaCl to saturate all exchange sites with  $\text{Na}^+$ . After again washing with de-ionized water the solid was dried at 333K for 3 days. The Na-4 mica powder sample was subjected to a  $\text{Pb}^{2+}2\text{Na}^+$  ion exchange reaction by immersing 2 g of powder into 25 ml of 0.4 (M)  $\text{Pb}(\text{NO}_3)_2$  to which 0.5 M NaCl solution was added. The reaction was carried out over a period of 4 weeks at 303 K with intermittent shaking. The ion-exchanged powder was separated from the solution by a centrifuge. The former was then heated in  $\text{H}_2\text{S}$  environment at 673 K for 1 h. This led to the formation of PbS wires within the nanochannels of Na-4 mica. The method of synthesis ensures that PbS is formed only within the crystal channels of Na-4 mica because of the presence of  $\text{Pb}^{2+}$  ions in them. There is no possibility of PbS being present on the surface of Na-4 mica. The melting point of PbS is 1387 K which is more than double the temperature used for the sulphidation treatment (673 K). Hence the probability of PbS evaporating during the treatment is very low. From the molecular formulas of Na-4 and PbS we have calculated the weight ratio between PbS and mica to be  $\sim 0.63$ .

The x-ray diffraction pattern of the composite was recorded in a Rich Seifert x-ray diffractometer 3000P (Ahrensburg, Germany) using  $\text{Cu } K\alpha$  radiation. The microstructure was studied by a JEOL model JEM 2010 transmission electron microscope (TEM). For this the specimen was ground in an agate mortar so that fine powders were produced. A small amount of this powder was taken in a test tube filled with acetone. The test tube was placed in an ultrasonic bath for 20 min to obtain a fine dispersion of the powder. One drop of

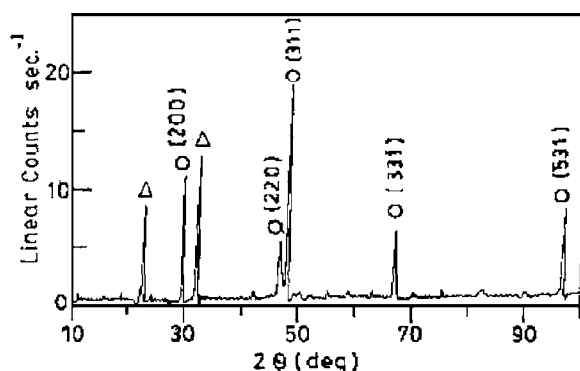


FIG. 1. X-ray diffractogram of PbS nanowires grown within Na-4 mica: ( $\Delta$ ) Na-4 mica and (O) PbS.

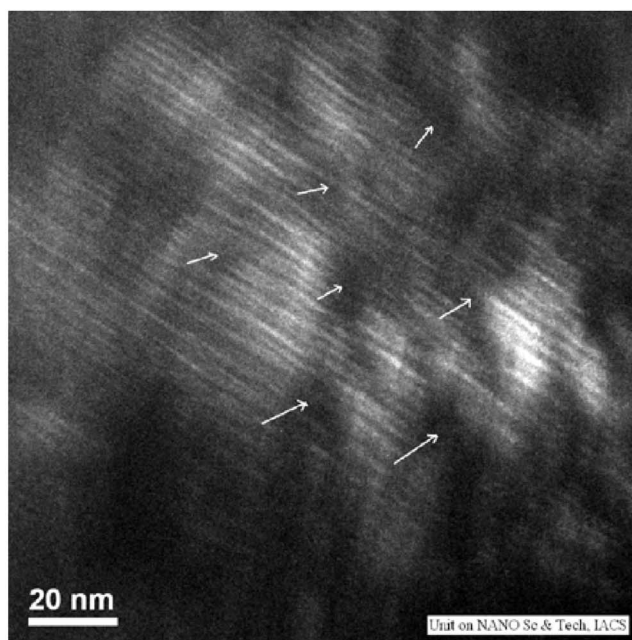
this dispersion was then placed on a carbon-coated grid (supplied by Polaron, UK). Acetone evaporated within few minutes, and the grid was mounted in the electron microscope chamber.

For electrical resistivity measurements specimens of 1 cm diameter and 1 mm thickness were prepared by compacting the powder at room temperature with a pressure of 20 tons/cm<sup>2</sup>. In order to avoid any grain boundary effect on the measured electrical properties the compacted specimen was subjected to a sintering treatment at 973 K for 1 h in a nitrogen atmosphere. Silver paste supplied by B.V. Colloiden, Netherlands, was applied on both the faces of the sintered samples to serve as electrodes. Voltage-current characteristics were measured at different temperatures using a Keithley 617 Electrometer. Dielectric measurements were also carried out in the frequency range from 1 kHz to 1.5 MHz by a Hewlett-Packard impedance analyzer (HP 4192A). It should be mentioned that the resistance behavior of the composites studied here is determined solely by PbS because the resistance of the pristine mica is several orders of magnitude higher than that of the composite. This should be evident from Figs. 4 and 5 as shown below.

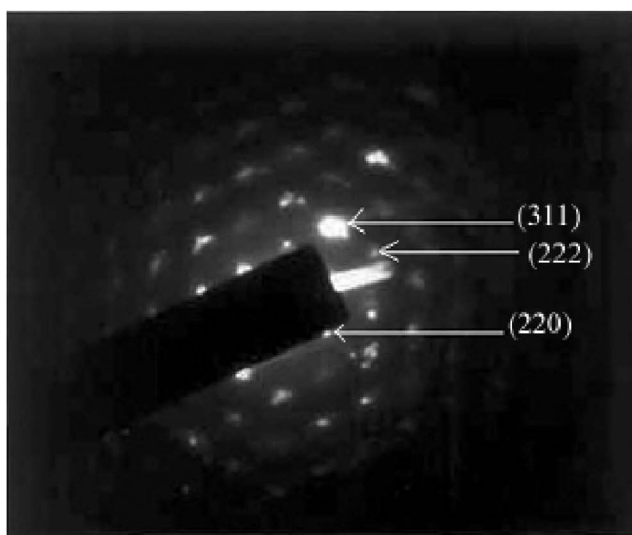
## RESULTS AND DISCUSSION

Figure 1 shows the x-ray diffractogram of the Na-4 sample in which PbS has been grown. It is evident that both Na-4 mica and PbS are present in the composite. A close examination of the peak intensities for PbS phase indicates that these bear a relation with respect to each other which is different from that given in the Data Handbook for randomly oriented powder of the same phase. For instance, the (311) peak has higher intensity than those obtained for (200) and (220) peaks, whereas the data handbook shows (200) and (220) to be 100% and 57% lines, respectively, and (311) to be 35%. This implies that PbS crystals have grown within the mica channels with the axis of the crystals aligned parallel to the channel. In such a situation the (200) and (220) planes will contribute much less to x-ray diffraction than the (311) plane. The TEM results as discussed below are consistent with the above observation.

Figure 2(a) is a dark field image of the transmission electron micrograph of the sample. The bright lines represent the



(a)



(b)

FIG. 2. (a) Dark field image of TEM micrograph for PbS/Nano-4 mica nanocomposite showing break gaps in PbS nanowires within a mica grain. (b) Electron diffraction pattern of micrograph corresponding to (a).

nanowires, and it is evident that many of the nanowires have break—gaps—some of these are indicated by the arrows *G*. Figure 2(b) is the electron diffraction pattern corresponding to Fig. 2(a) which is typical of all the composites. The interplanar spacings ( $d_{hkl}$ ) calculated from the diffraction spots are summarized in Table I and are compared with ASTM values for PbS. It is evident that the values are in satisfactory agreement, confirming that PbS single crystalline nanowires have formed. We have marked the ( $hkl$ ) values to the diffraction spots in Fig. 2(b). The diameter of the nanowires is estimated from Fig. 2(a) to be  $\sim 1.2$  nm. This is consistent with the interlayer spacing in Na-4 mica.<sup>15</sup> In Fig. 3 we show dark field images of two grains which exhibit that some of

TABLE I. Comparison of interplanar spacings  $d_{hkl}$  obtained from electron diffraction pattern of nanocomposite with standard ASTM data.

Observed (nm)	Standard PbS (nm)
0.203	0.2099(220)
0.179	0.1790(311)
0.172	0.171(222)
0.136	0.1362(331)
0.112	0.114(511)
0.108	0.1048(440)

the nanowires are continuous between the grains (shown by arrow *C*) whereas the rest have discontinuities at the grain boundary. The lines have been drawn in the figure to denote the grain boundary. From the x-ray diffractogram of Fig. 1 we determined the average particle size of Na-4 crystallites using Scherrer's equation.<sup>19</sup> This was found to be 44 nm. It can therefore be concluded from the micrograph of Fig. 2(a) that there are ruptured PbS strands of length  $\sim 20$  nm present within the mica-4 grains. It is probable therefore that in the present specimen system there is a percolating fraction of nanowires which will participate in electrical conduction.

In Fig. 4 we show the variation of  $\log_{10}\rho$  as a function of inverse temperature for a specimen of compacted Na-4 mica. It is evident that the resistivity varies from  $10^{10}$  to  $10^{12}$   $\Omega$  cm in the temperature range 370–307 K. The resistivity of pristine mica is several orders of magnitude higher than those of the composites containing PbS as shown below.

Figure 5 shows the variation of resistivity as a function of temperature for the composite of Na-4 mica and PbS nanowires. The resistivity was estimated from the slope of voltage-current characteristics measured at low voltages. It is

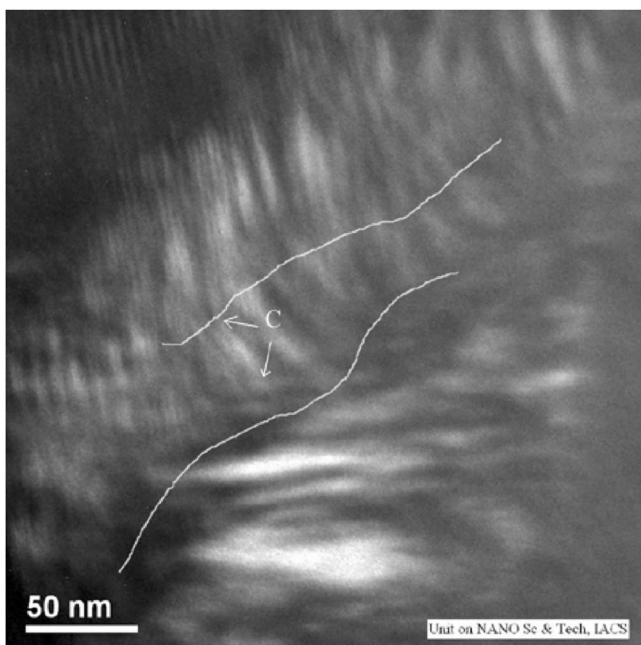


FIG. 3. Dark field TEM image of two grains of mica containing PbS nanowires.

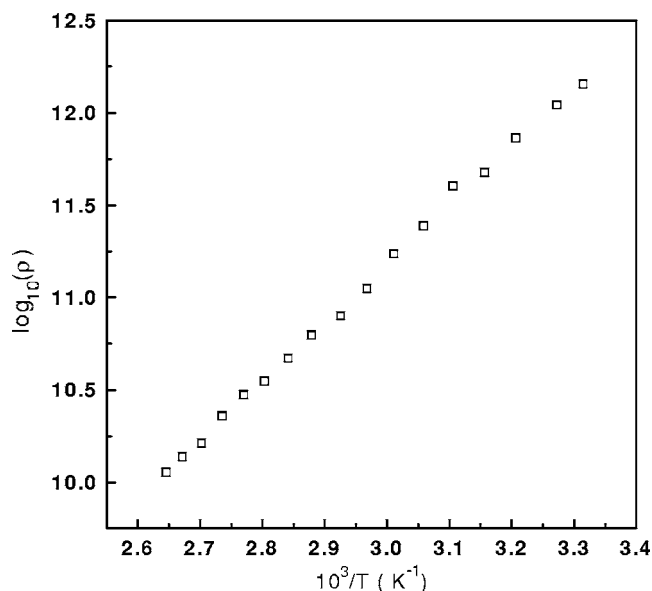


FIG. 4.  $\log_{10}\rho$  as a function of inverse temperature for a Na-4 specimen (compacted powder).

evident that there is a transition from semiconducting to metallic behavior at around 300 K as the temperature is lowered. Measurements were carried out on two different samples prepared by identical procedure as mentioned above. The results—viz., the resistivity values, the transition temperature, and dielectric constant values (reported below)—were reproducible to within 2%. The temperature variation of electrical resistivity for a semiconductor should follow a relation<sup>20</sup>

$$\rho \propto \exp(E_g/2kT), \tag{1}$$

where  $E_g$  is the band gap and  $k$  the Boltzmann constant. We have therefore plotted  $\log_e\rho$  against  $T^{-1}$  using data for temperatures higher than 300 K in Fig. 6. The line in this figure

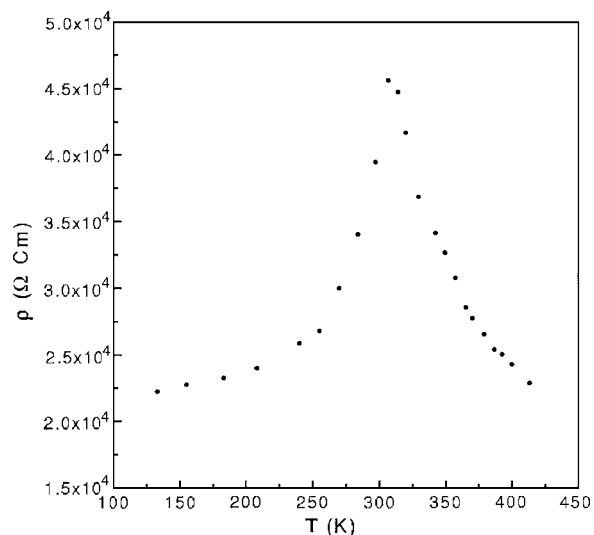


FIG. 5. Resistivity variation as a function of temperature for PbS/Na-4 mica nanocomposite.

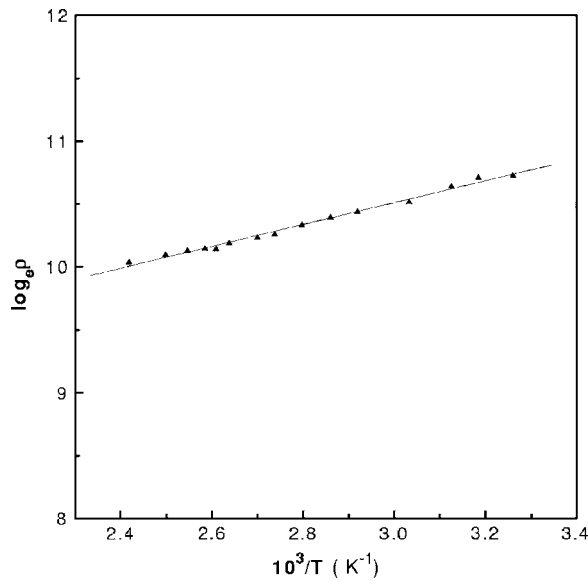


FIG. 6.  $\log_e \rho$  vs  $T^{-1}$  for PbS/Na-4 mica nanocomposite at temperatures above 300 K: ( $\Delta$ ) experimental data and (solid line) straight line fitting.

is the theoretical fit and a value of  $E_g = 0.32$  eV is extracted. This value pertains to PbS.<sup>17</sup> It may be mentioned here that the quasi-one-dimensional semiconductors exhibit a band gap similar to that of their bulk counterpart.<sup>21</sup> The transition to a metallic state is ascribed to a pressure-induced one. This pressure is generated because of the mismatch of thermal expansions of mica and PbS phases. The values are  $80 \times 10^{-6}/\text{K}$  and  $19 \times 10^{-6}/\text{K}$ , respectively.<sup>22</sup> Taking the bulk modulus value of PbS to be  $\sim 12.7 \times 10^{10}$  Pa,<sup>19</sup> we calculate a pressure of  $\sim 3.1$  GPa which is effective when the sample is cooled from 673 K to room temperature. It may be mentioned here that a structural transition has been observed earlier in the case of PbS nanoparticles subjected to a hydrostatic pressure of the order of 6 GPa.<sup>23</sup> The resistivity change was explained as arising due to a decrease of energy band gap with increasing pressure. It is therefore concluded that in our sample system the semiconductor-metal transition is brought about by a high-pressure effect caused by the thermal mismatch of the nanotemplate (Na-4 mica) and the PbS nanowire grown within the channels of the former.

In Fig. 7 is shown the voltage-current characteristics of the sample at different temperatures below 300 K. The curves are nonlinear but symmetrical (with respect to voltage). This is due to the presence of an array of metal-semiconductor junctions. The portion of PbS within a mica grain will be subjected to high pressure and therefore undergo a semiconductor-metal transition whereas the portion at the interface between grains (shown by  $C$  in Fig. 3) will not experience any high pressure and therefore retain its semiconducting characteristics. The current flow  $I$  is given by<sup>24</sup>

$$I = I_0 [\exp(eV/kT) - 1], \quad (2)$$

where  $I_0$  is the saturation current,  $e$  is the electronic charge, and  $V$  is the applied voltage. For small voltage the above

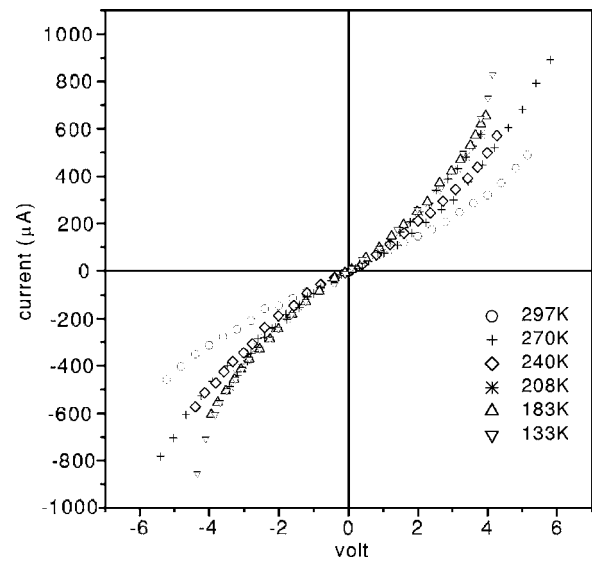


FIG. 7. Voltage-current characteristics of PbS/Na-4 nanocomposite at temperatures below 300 K: (O) 297 K+270 K, ( $\diamond$ ) 240 K, (\*) 208 K, ( $\Delta$ ) 183 K, and ( $\nabla$ ) 133 K.

equation reduces to  $I = I_0 eV/kT$  which will show a lowering of resistivity as the temperature is reduced.

However, there is a change of slope in the  $\rho$ - $T$  plot at temperatures below  $\sim 240$  K. We explain this as follows.

The calculated value of intrinsic resistivity of PbS (Ref. 19) at 300 K is  $\sim 100 \Omega \text{ cm}$ . The value measured by us at this temperature for the semiconducting state of PbS is, however, of the order of  $4 \times 10^4 \Omega \text{ cm}$ . This means there is a discrepancy of the order of  $\sim 10^2$ . This arises because of the small number of percolative paths of PbS nanowires existing in these composites as already mentioned above. Evidently, the areal fraction covered by these nanowires will be  $\sim 0.005$ . Taking the diameter of a nanowire to be equal to 1.2 nm as pointed out before, it turns out that the number of nanowires which are percolative in our system is  $\sim 3.5 \times 10^9$ . The areal fraction covered by ruptured PbS nanowires [as pointed out in Fig. 2(a)] will therefore be  $\sim 0.995$ . Therefore after the transition has occurred these nanowires will control the electrical behavior. These nanowires will have two types of junctions—one at the interface between the grains and the other within the grain at the ruptured portion. The change of slope in the resistivity temperature plot therefore occurs when the effect of the intragranular junction becomes dominant.

Figure 8 shows the variation of dielectric constant as a function of temperature for a PbS/Na-4 mica nanocomposite. The values shown in the figure were obtained from the high-frequency (1.5 MHz) dielectric measurements. There is a sharp transition in dielectric constant at around 300 K. A giant dielectric permittivity around 280 is found at lower temperatures whereas a value of  $\sim 21$  is recorded at temperatures higher than 300 K. This is explained as arising due to metallic strands formed as a result of the semiconductor-metal transition in PbS. For the one-dimensional metallic system it was earlier shown that the dielectric constant is given by<sup>14</sup>

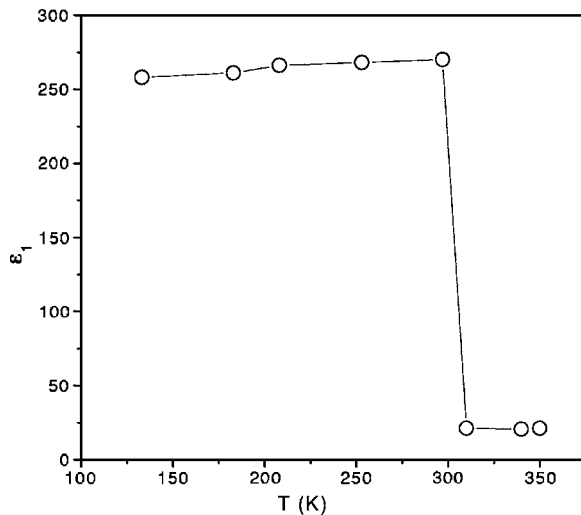


FIG. 8. Variation of dielectric constant as a function of temperature for a PbS/Na-4 mica nanocomposite.

$$\varepsilon \cong \frac{1}{2}(l_0 q_s)^2, \quad (3)$$

where  $l_0$  is the average length of a metallic strand and  $q_s$  is the Fermi-Thomas screening wave vector of the conduction electrons. For metallic densities  $q_s \sim a^{-1}$  where  $a$  is the interatomic distance of the metal phase. Taking  $a \sim 0.59$  nm (Ref. 22) and putting  $l_0 \sim 20$  nm [this value is estimated from the electron micrograph in Fig. 2(a)], we estimate a value of  $\varepsilon \cong 570$ . The estimated value is of the same order as that measured. However, there is a quantitative discrepancy. This could be due to the fact that not all the grains containing

the PbS nanowires contribute to polarizability enhancement because of the random alignment of the grains and therefore the nanowires with respect to the direction of the applied electric field. Also, there is a distribution of grain sizes within the sample, thereby implying that there are grains smaller than 20 nm which could have a larger influence on the dielectric response of the composite samples.

In summary, PbS nanowires of diameter 1.2 nm have been grown within the crystal channels of Na-4 mica. A semiconductor to metal transition has been observed at a temperature around 300 K. This has been ascribed to the generation of a pressure  $\sim 3$  GPa on PbS nanowires due to thermal expansion mismatch of Na-4 mica and PbS phases, respectively. Voltage-current characteristics at different temperatures below 300 K show nonlinear behavior. This arises due to the formation of nanojunctions between the metallic phases and the untransformed regions of PbS nanowires. A transition from a high value ( $\sim 280$ ) to a low one ( $\sim 21$ ) of dielectric constant was found at a temperature of 300 K. This is consistent with a semiconductor to metal transition in the case of PbS. The high value of dielectric constant exhibited by the nanocomposites is a consequence of the Rice-Bernasconi mechanism of dielectric polarizability in broken one-dimensional conductors.

#### ACKNOWLEDGMENTS

The work has been carried out under the Nano Science and Technology Initiative Programme of Department of Science and Technology, New Delhi. D. C. acknowledges the Indian National Science Academy, New Delhi, for support. The authors thank Supriya Chakraborty for help with electron microscopy and Soumen Basu in the preparation of the manuscript.

- <sup>1</sup>Y. Xia, P. Yang, Y. Sun, Y. Wu, B. Mayers, B. Gates, Y. Yin, F. Kim, and H. Yan, *Adv. Math.* **15**, 353 (2003).
- <sup>2</sup>M. Huang, S. Mao, H. Feick, H. Yan, Y. Wu, H. Kind, E. Weber, R. Russo, and P. Yang, *Science* **292**, 2897 (2001).
- <sup>3</sup>P. Yang, Y. Wu, and R. Fan, *Int. J. Nanosci.* **1**, 1 (2002).
- <sup>4</sup>C. N. R. Rao and A. G. Govindaraj, *Acc. Chem. Res.* **35**, 998 (2002).
- <sup>5</sup>W. Han, S. Fan, Q. Li, and Y. Hu, *Science* **277**, 1287 (1997).
- <sup>6</sup>C. R. Martin, *Science* **266**, 1961 (1994).
- <sup>7</sup>Y. Xia, J. A. Rogers, K. Paul, and G. M. Whitesides, *Chem. Rev.* **99**, 1823 (1999).
- <sup>8</sup>S. Bhattacharyya, S. K. Saha, and D. Chakravorty, *Appl. Phys. Lett.* **77**, 3770 (2000).
- <sup>9</sup>P. M. Ajayan, O. Stephan, P. Redlich, and C. Colliox, *Nature (London)* **375**, 564 (1995).
- <sup>10</sup>D. Routkevich, T. Bigioni, M. Moskovits, and J. M. Xu, *J. Phys. Chem.* **100**, 14037 (1996).
- <sup>11</sup>Z. Zhang, J. Y. Ying, and M. S. Dresselhaus, *J. Mater. Res.* **13**, 1745 (1998).
- <sup>12</sup>P. K. Mukherjee and D. Chakravorty, *J. Mater. Res.* **17**, 3127 (2002).
- <sup>13</sup>L. P. Gorkov and G. M. Eliashberg, *Sov. Phys. JETP* **21**, 940 (1965).
- <sup>14</sup>M. J. Rice and J. Bernasconi, *Phys. Rev. Lett.* **29**, 113 (1972).
- <sup>15</sup>R. Kubo, *J. Phys. Soc. Jpn.* **17**, 975 (1962).
- <sup>16</sup>R. Dupree and M. A. Smithard, *J. Phys. C* **5**, 408 (1972).
- <sup>17</sup>F. Meier and P. Wyder, *Phys. Lett.* **39A**, 51 (1972).
- <sup>18</sup>T. Kodama and S. Komarneni, *J. Mater. Chem.* **9**, 533 (1999).
- <sup>19</sup>H. P. Klug and L. E. Alexander, *X-ray Diffraction Procedures for Polycrystalline and Amorphous Materials* (Wiley Interscience, New York, 1974), p. 689.
- <sup>20</sup>C. Kittel, *Introduction to Solid State Physics* (Wiley, London, 1961), p. 351.
- <sup>21</sup>*Metal and Semiconductor Nanowires, Vol. 1 of Nanowires and Nanobelts*, edited by Z. L. Wang (Kluwer Academic, Norwell, MA, 2003).
- <sup>22</sup>*American Institute of Physics Handbook*, edited by D. E. Gray (McGraw Hill, New York, 1957).
- <sup>23</sup>J. Z. Jiang *J. Appl. Phys.* **87**, 2658 (2000).
- <sup>24</sup>C. Kittel, *Introduction to Solid State Physics* (Wiley, New York 1961), p. 389.